Investigation of Solid-State Forms between p-Aminosalicylic Acid and Adenine: Exploring Salts, Cocrystals and their Polymorphism

Beatrice Maiorca,[a] Chiara Sabena,[a] Emanuele Priola,[a] Ilenia D'Abbrunzo, [b] Beatrice Perissutti,[b] Roberto Gobetto,[a,*] Michele R. Chierotti [a,*]

[a] Department of Chemistry, University of Torino, 10125 Torino, Italy

[b] Department of Chemical and Pharmaceutical Sciences, University of Trieste, P.le Europa 1, 34127, Trieste, Italy

* Corresponding authors. *E-mail address:* michele.chierotti@unito.it and roberto.gobetto@unito.it

Supplementary Material

Table S1 - Crystal data and structure refinement for the adducts PAS-ADE Form B and C.

	Form B	Form C
Empirical formula	$C_{12}H_{16}N_6O_5$	$C_{12}H_{16}N_6O_5$
Formula weight	324.31	324.31
Temperature/K	293.00	298.00
Crystal system	orthorhombic	triclinic
Space group	Fdd2	P-1
a/Å	34.2161(8)	8.0819(11)
b/Å	25.2032(4)	8.8634(8)
c/Å	6.93342(12)	11.0867(12)
α/°	90	80.382(8)
β/°	90	68.789(11)
γ/°	90	80.165(9)
Volume/Å^3	5979.1(2)	724.70(15)
Z	16	2
ρ_{calc}g/cm^3	1.441	1.486
μ/mm^{-1}	0.976	1.007
F(000)	2720.0	340.0
Crystal size/mm^3	0.12 × 0.11 × 0.1	0.12 × 0.1 × 0.09
Radiation	CuKα (λ = 1.54184)	CuKα (λ = 1.54184)
2Θ range for data collection/°	8.716 to 133.59	8.612 to 134.202
Index ranges	-35 ≤ h ≤ 39, -29 ≤ k ≤ 30, -6 ≤ l ≤ 8	-9 ≤ h ≤ 8, -10 ≤ k ≤ 10, -12 ≤ l ≤ 13
Reflections collected	11234	5459
Independent reflections	2331 [R_{int} = 0.0251, R_{sigma} = 0.0204]	2440 [R_{int} = 0.0417, R_{sigma} = 0.0292]
Data/restraints/parameters	2331/1/228	2440/0/216
Goodness-of-fit on F^2	1.065	1.050
Final R indexes [I>=2σ (I)]	R_1 = 0.0298, wR_2 = 0.0778	R_1 = 0.0552, wR_2 = 0.1547
Final R indexes [all data]	R_1 = 0.0318, wR_2 = 0.0795	R_1 = 0.0586, wR_2 = 0.1624
Largest diff. peak/hole / e Å^{-3}	0.14/-0.14	0.35/-0.30
Flack parameter	0.10(12)	

Table S2 - Bond Lengths for the adduct PAS-ADE Form B.

Atom	Atom	Length/Å	Atom	Atom	Length/Å
N3	C8	1.368(3)	O1	C3	1.366(3)
N3	C12	1.351(3)	C2	C7	1.403(3)
C11	N4	1.356(3)	C2	C3	1.409(3)
C11	C9	1.387(3)	C2	C1	1.466(4)
C11	N5	1.358(3)	O3	C1	1.263(3)
N4	C12	1.306(3)	C5	C6	1.403(3)
C9	C8	1.392(3)	C5	C4	1.391(4)
C9	N6	1.381(3)	C5	N1	1.356(4)
N2	C8	1.321(3)	C6	C7	1.366(4)
N6	C10	1.318(3)	O2	C1	1.277(3)
N5	C10	1.359(3)	C3	C4	1.377(4)

Table S3 - Bond Angles for the adduct PAS-ADE Form B.

Atom	Atom	Atom	Angle/°	Atom	Atom	Atom	Angle/°
C12	N3	C8	123.1(2)	C7	C2	C3	117.1(2)
N4	C11	C9	127.3(2)	C7	C2	C1	121.0(2)
N4	C11	N5	127.1(2)	C3	C2	C1	121.9(2)
N5	C11	C9	105.6(2)	C4	C5	C6	118.6(2)
C12	N4	C11	111.9(2)	N1	C5	C6	119.7(2)
C11	C9	C8	117.6(2)	N1	C5	C4	121.8(2)
N6	C9	C11	110.5(2)	C7	C6	C5	120.5(2)
N6	C9	C8	131.8(2)	C6	C7	C2	121.9(2)
N3	C8	C9	114.5(2)	O1	C3	C2	120.7(2)
N2	C8	N3	118.2(2)	O1	C3	C4	118.2(2)
N2	C8	C9	127.3(2)	C4	C3	C2	121.1(2)
C10	N6	C9	103.7(2)	O3	C1	C2	120.3(2)
C11	N5	C10	106.7(2)	O3	C1	O2	121.9(2)
N6	C10	N5	113.4(2)	O2	C1	C2	117.8(2)
N4	C12	N3	125.6(2)	C3	C4	C5	120.8(2)

Table S4 - Bond Lengths for the adduct PAS-ADE Form C.

Atom	Atom	Length/Å	Atom	Atom	Length/Å
O1	C1	1.259(2)	N2	C8	1.314(2)
O2	C1	1.2777(19)	N4	C11	1.362(2)
N3	C12	1.351(2)	N4	C12	1.298(2)
N3	C8	1.356(2)	C11	N5	1.355(2)
O3	C7	1.3568(19)	C7	C6	1.385(2)
C2	C1	1.474(2)	N5	C10	1.355(2)
C2	C7	1.404(2)	C5	C6	1.397(2)
C2	C3	1.401(2)	C5	N1	1.365(2)
C9	C11	1.385(2)	C5	C4	1.399(2)
C9	N6	1.375(2)	N6	C10	1.310(2)
C9	C8	1.406(2)	C4	C3	1.369(2)

Table S5 - Bond Angles for the adduct PAS-ADE Form B.

Atom	Atom	Atom	Angle/°	Atom	Atom	Atom	Angle/°
C12	N3	C8	123.18(14)	O3	C7	C6	117.05(15)
C7	C2	C1	121.76(14)	C6	C7	C2	121.38(15)
C3	C2	C1	121.28(15)	C11	N5	C10	106.31(14)
C3	C2	C7	116.96(15)	C6	C5	C4	118.85(15)
C11	C9	C8	117.97(15)	N1	C5	C6	121.10(17)
N6	C9	C11	110.36(14)	N1	C5	C4	120.03(16)
N6	C9	C8	131.66(15)	C10	N6	C9	103.74(14)
O1	C1	O2	122.32(15)	C7	C6	C5	120.33(16)
O1	C1	C2	120.81(14)	N4	C12	N3	126.21(16)
O2	C1	C2	116.87(14)	N3	C8	C9	114.10(14)
C12	N4	C11	111.86(14)	N2	C8	N3	119.48(15)
N4	C11	C9	126.66(15)	N2	C8	C9	126.42(16)
N5	C11	C9	105.79(14)	C3	C4	C5	120.13(15)
N5	C11	N4	127.54(14)	N6	C10	N5	113.80(16)
O3	C7	C2	121.56(15)	C4	C3	C2	122.34(16)

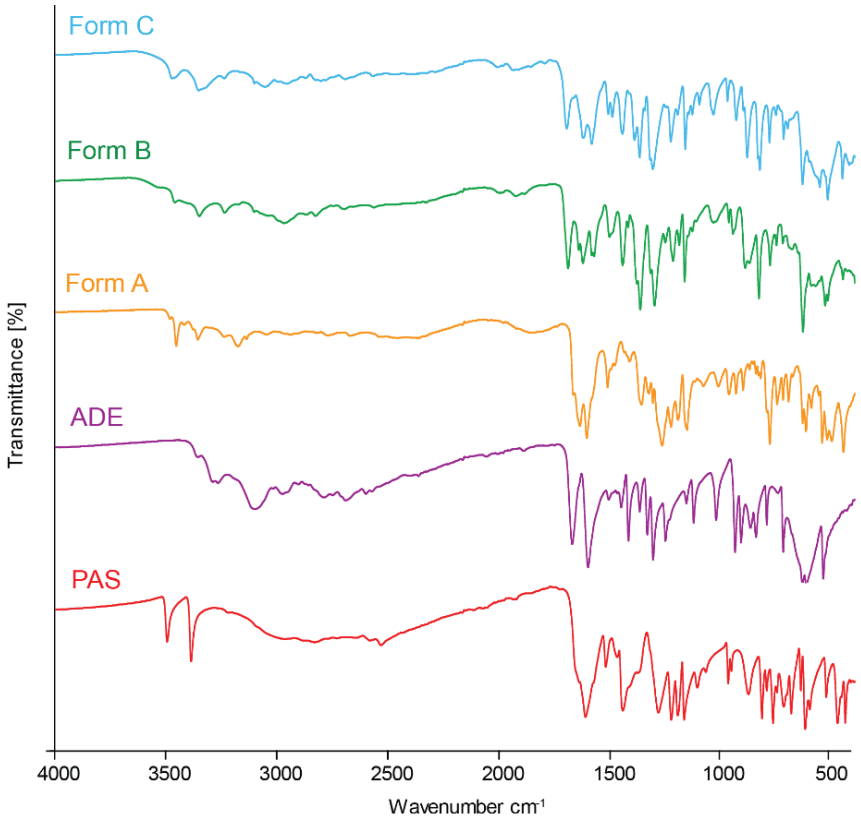

Figure S1 - Comparison among FTIR-ATR (4000-550 cm^{-1}) spectra of PAS, ADE and Form A, B and C.

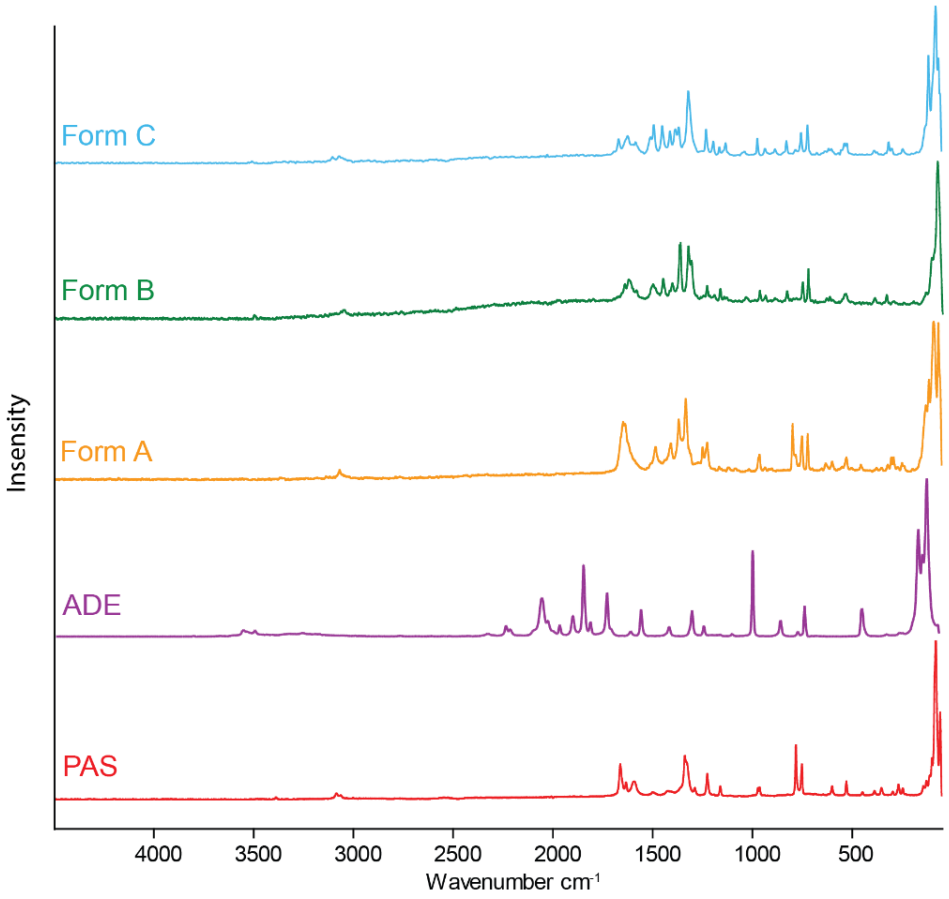

Figure S2 - Comparison among Raman Spectra of PAS, ADE and Form A, B, and C.

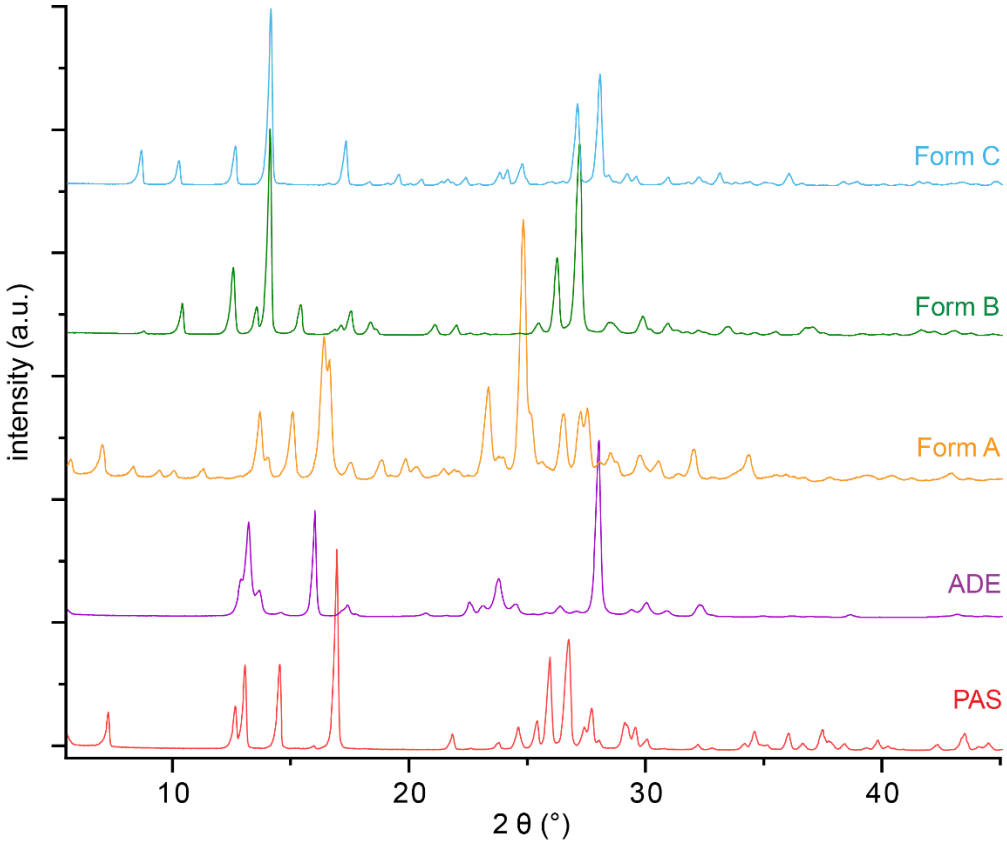

Figure S3 - Comparison among PXRD patterns of PAS, ADE and Form A, B and C.

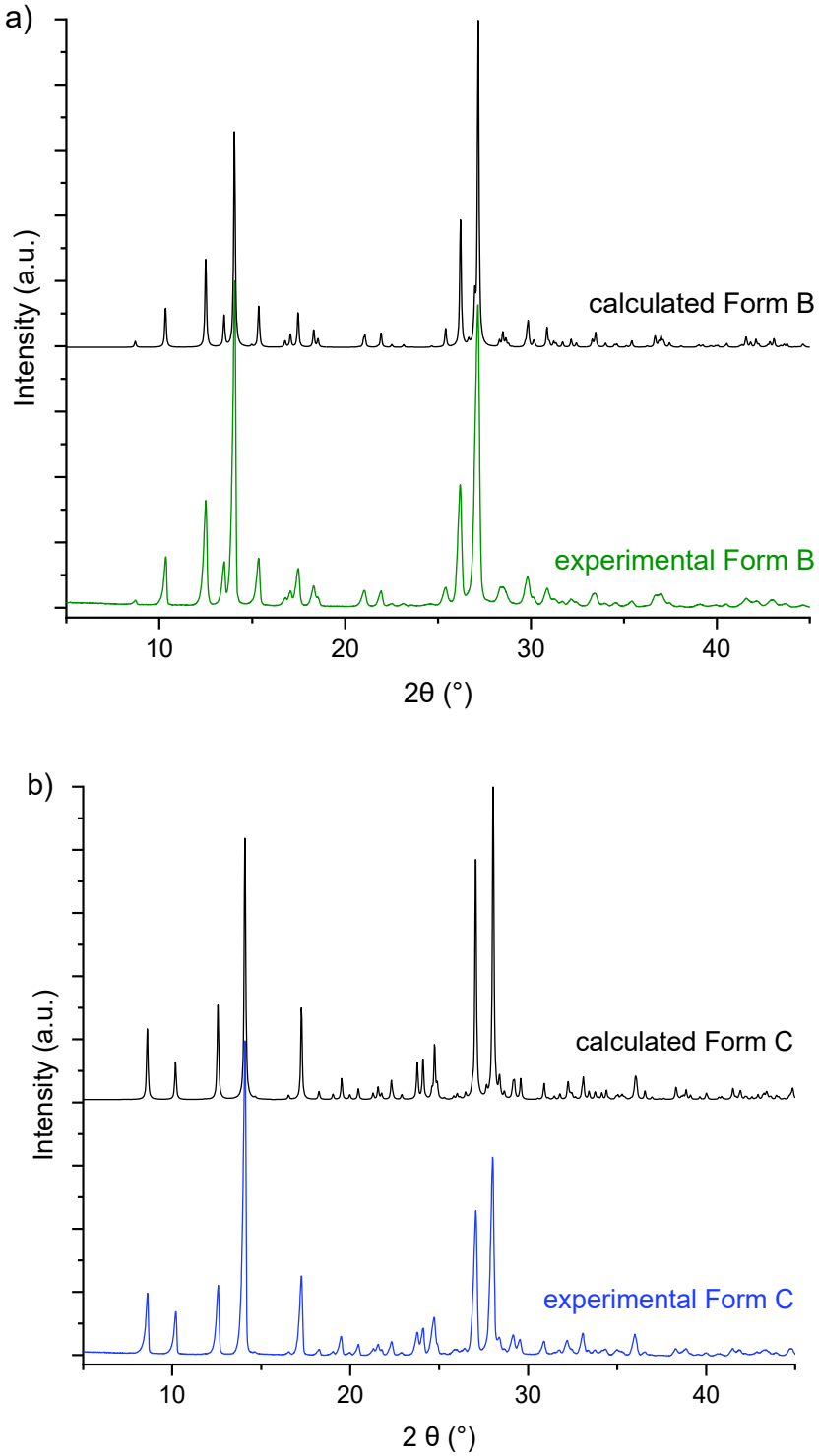

Figure S4 - Comparison between experimental and calculated PXRD patterns of Form B (a) and Form C (b).

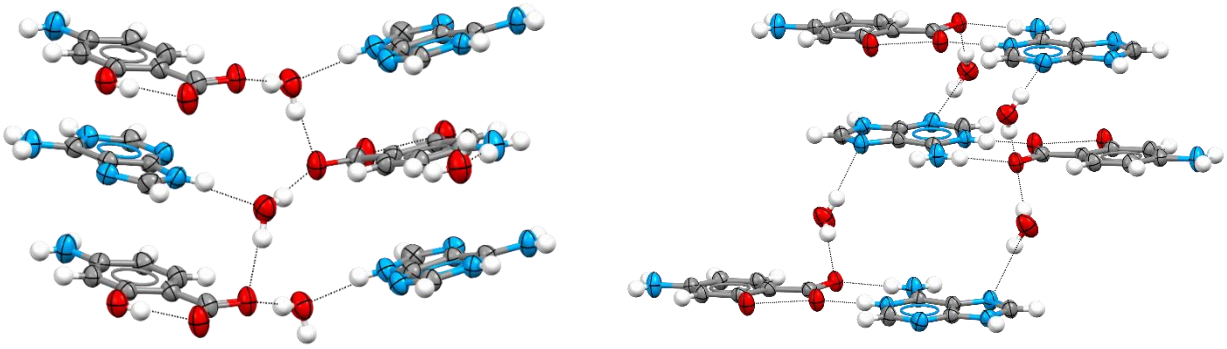

Figure S5 - Fragments of the crystal packing of form B (left) and of form C (right) highlighting the role of the water molecules in linking columns (Form B) and layers (Form C). (Ellipsoid probability: 70%). Color code: grey, carbon; blue, nitrogen; red, oxygen; white, hydrogen.

Table S6 - Pairwise interaction energies and their main components calculated for Form B. Corresponding molecules are distinguished by different colors (in the Figure below).

	N	Symop	R	Electron Density	E_ele	E_pol	E_dis	E_rep	E_tot
	0	-	3.98	B3LYP/6-311G(d,p)	5.6	-0.4	-1.1	0.3	
	0	-	4.79	B3LYP/6-311G(d,p)	-70.4	-19.9	-5.8	53.1	
	0	-	4.23	B3LYP/6-311G(d,p)	1.2	-3.8	-6.7	8.5	
	0	-x, -y, -z	4.77	B3LYP/6-311G(d,p)	-1.8	-0.1	-0.3	0.0	
	0	-	4.42	B3LYP/6-311G(d,p)	-67.8	-21.4	-7.5	48.8	
	0	-	6.44	B3LYP/6-311G(d,p)	13.4	-3.2	-1.5	0.2	
	0	-	4.72	B3LYP/6-311G(d,p)	-8.7	-3.2	-7.2	27.1	
	0	-	5.80	B3LYP/6-311G(d,p)	7.1	-0.9	-1.6	0.2	
	0	-	6.01	B3LYP/6-311G(d,p)	-21.6	-3.6	-2.9	4.1	
	0	-x, -y, -z	9.63	B3LYP/6-311G(d,p)	152.3	-6.3	-1.3	0.0	
	0	-	8.31	B3LYP/6-311G(d,p)	-135.2	-8.4	-7.4	4.5	
	0	-	6.72	B3LYP/6-311G(d,p)	-226.7	-29.2	-10.4	21.4	
	0	-x, -y, -z	5.86	B3LYP/6-311G(d,p)	196.6	-15.8	-13.6	8.1	

0	x, y, z	8.86	B3LYP/6-311G(d,p)	154.5	-5.8	-1.8	0.1	
0	-	6.01	B3LYP/6-311G(d,p)	-21.6	-3.6	-2.9	4.1	
0	-	4.27	B3LYP/6-311G(d,p)	-18.4	-3.1	-7.1	33.1	
0	-	6.61	B3LYP/6-311G(d,p)	-181.2	-10.5	-9.7	7.9	
0	-	4.79	B3LYP/6-311G(d,p)	-70.4	-19.9	-5.8	53.1	
0	-	4.01	B3LYP/6-311G(d,p)	-287.9	-39.4	-33.5	21.7	
0	-	7.26	B3LYP/6-311G(d,p)	-474.2	-100.2	-13.9	135.6	
0	-x, -y, -z	6.49	B3LYP/6-311G(d,p)	243.8	-24.5	-8.4	0.9	
0	-	4.72	B3LYP/6-311G(d,p)	-8.7	-3.2	-7.2	27.1	
0	-	6.44	B3LYP/6-311G(d,p)	13.4	-3.2	-1.5	0.2	
0	-	5.56	B3LYP/6-311G(d,p)	-4.1	-4.1	-3.1	2.6	
0	-	7.14	B3LYP/6-311G(d,p)	15.4	-2.2	-0.8	0.0	
0	-	4.20	B3LYP/6-311G(d,p)	-276.6	-38.0	-36.7	26.6	
2	x, y, z	8.86	B3LYP/6-311G(d,p)	163.5	-10.4	-2.0	0.3	
1	-	4.01	B3LYP/6-311G(d,p)	-287.9	-39.4	-33.5	21.7	
1	-	7.26	B3LYP/6-311G(d,p)	-474.2	-100.2	-13.9	135.6	
1	-	4.42	B3LYP/6-311G(d,p)	-67.8	-21.4	-7.5	48.8	
1	-	5.24	B3LYP/6-311G(d,p)	-18.2	-3.9	-4.6	2.7	
1	-	4.26	B3LYP/6-311G(d,p)	-53.3	-19.1	-8.5	40.0	
1	-	6.61	B3LYP/6-311G(d,p)	-181.2	-10.5	-9.7	7.9	
1	-	8.31	B3LYP/6-311G(d,p)	-135.2	-8.4	-7.4	4.5	
1	-	4.23	B3LYP/6-311G(d,p)	1.2	-3.8	-6.7	8.5	
1	-	6.17	B3LYP/6-311G(d,p)	-6.2	-3.0	-3.5	10.0	

	1	-	6.72	B3LYP/6-311G(d,p)	-226.7	-29.2	-10.4	21.4	
	1	-	5.80	B3LYP/6-311G(d,p)	7.1	-0.9	-1.6	0.2	
	1	-	5.50	B3LYP/6-311G(d,p)	-23.0	-3.6	-5.9	16.9	
	1	-x, -y, -z	5.84	B3LYP/6-311G(d,p)	325.5	-45.9	-13.9	7.2	
	1	-	4.20	B3LYP/6-311G(d,p)	-276.6	-38.0	-36.7	26.6	
	1	-x, -y, -z	7.45	B3LYP/6-311G(d,p)	125.8	-8.5	-8.7	7.0	
	1	-x, -y, -z	10.28	B3LYP/6-311G(d,p)	92.5	-1.0	-9.4	10.4	
	1	-x, -y, -z	7.17	B3LYP/6-311G(d,p)	159.9	-11.3	-3.6	0.6	

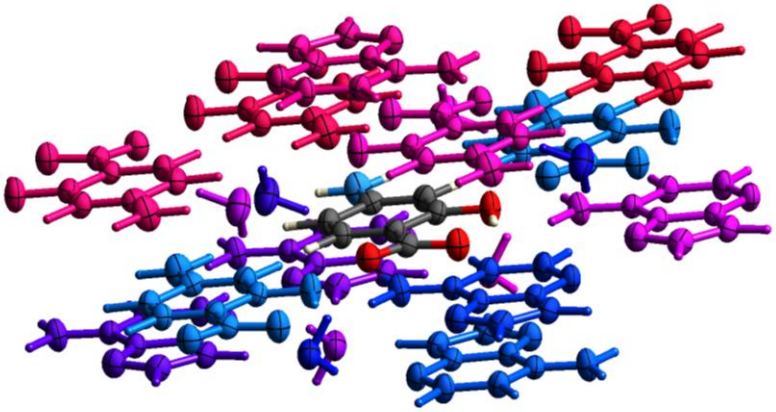

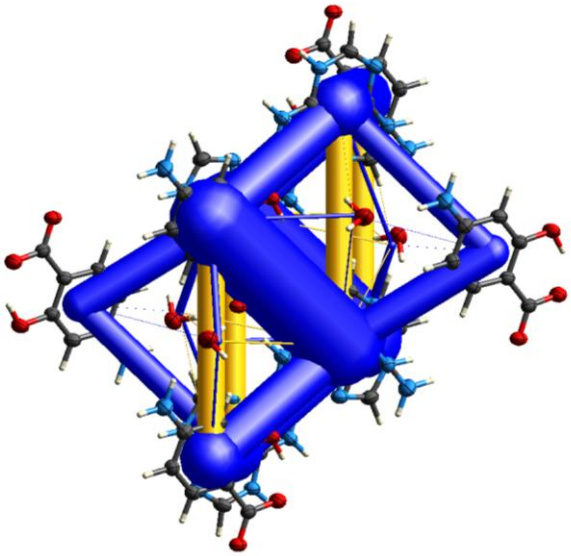

a)

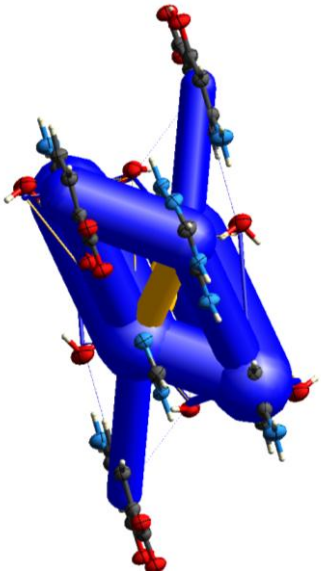

b)

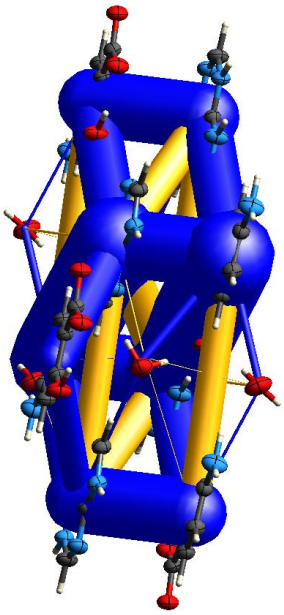

c)

Figure S6 - Total Energy component of Energy Framework of Form B along [100] (a), [010] (b) and [001] (c) (Color code: blue, attractive; yellow, repulsive).

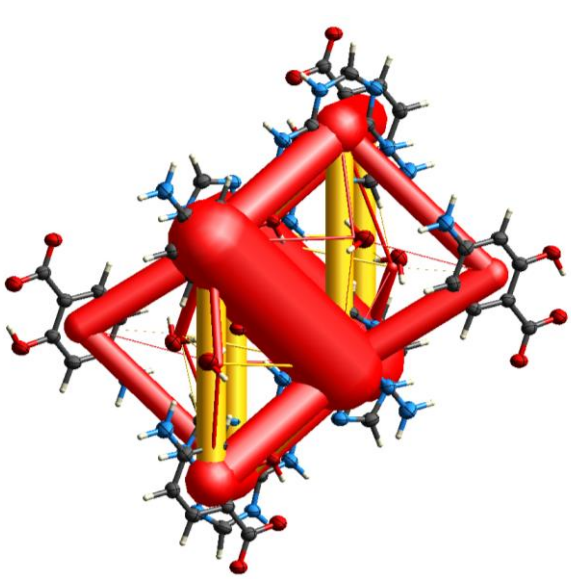

a)

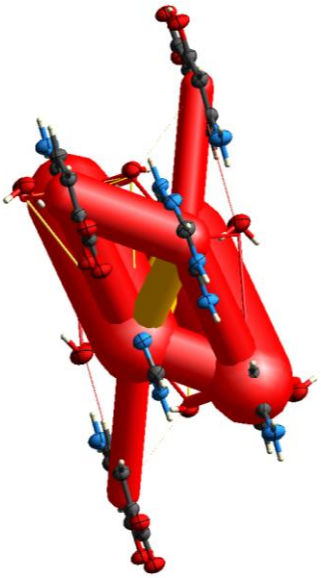

b)

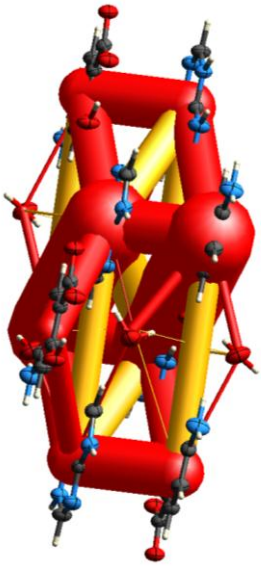

c)

Figure S7 - Coulombic component of Energy Framework of Form B along [100] (a), [010] (b) and [001] (c) (Color code: red, attractive; yellow, repulsive).

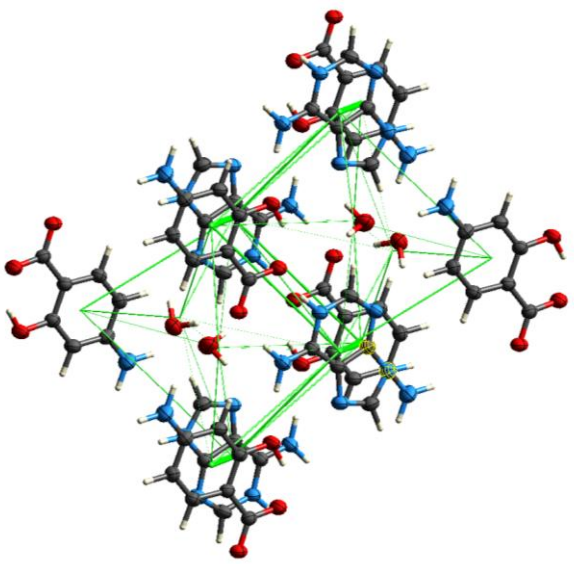

a)

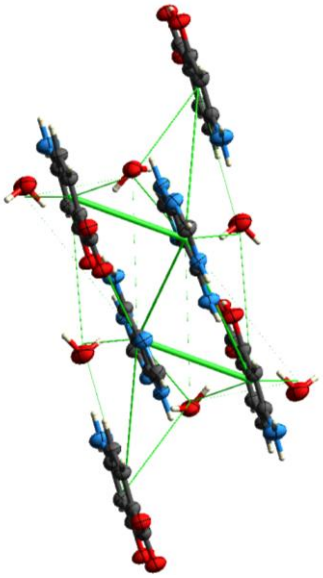

b)

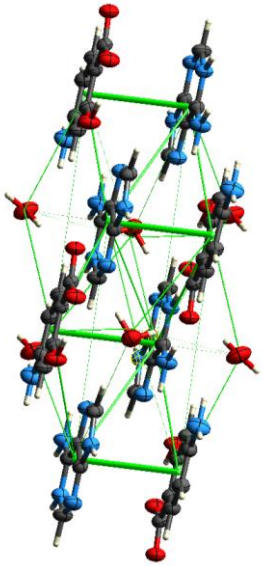

c)

Figure S8 - Dispersion component of Energy Framework of Form B along [100] (a), [010] (b) and [001] (c).

Table S7 - Pairwise interaction energies and their main components calculated for Form C. Corresponding molecules are distinguished by different colors (in the Figure below).

	N	Symop	R	Electron Density	E_ele	E_pol	E_dis	E_rep	E_tot
	0	-	4.73	B3LYP/6-311G(d,p)	-3.2	-2.7	-7.7	24.5	
	0	-	5.84	B3LYP/6-311G(d,p)	-3.5	-5.7	-4.3	9.8	
	0	-	4.59	B3LYP/6-311G(d,p)	-2.9	-4.7	-5.2	5.7	
	0	-	5.02	B3LYP/6-311G(d,p)	25.6	-3.1	-1.8	0.4	
	0	-	5.51	B3LYP/6-311G(d,p)	-23.7	-6.0	-7.3	35.0	
	0	-x+1/2, -y+1/2, z	3.29	B3LYP/6-311G(d,p)	3.7	-0.5	-1.9	1.4	
	0	-	5.03	B3LYP/6-311G(d,p)	9.4	-3.3	-3.3	1.3	
	0	-	6.16	B3LYP/6-311G(d,p)	-11.6	-2.8	-0.9	0.1	
	2	-x+1/4, y+3/4, z+3/4	6.62	B3LYP/6-311G(d,p)	163.2	-19.8	-12.1	34.9	
	2	x+1/4, -y+3/4, z+3/4	8.73	B3LYP/6-311G(d,p)	179.9	-8.8	-1.7	0.0	
	1	-	4.86	B3LYP/6-311G(d,p)	-63.9	-17.1	-5.3	40.0	
	1	-	4.01	B3LYP/6-311G(d,p)	-242.0	-32.3	-38.2	29.9	
	1	-	7.27	B3LYP/6-311G(d,p)	-184.5	-10.0	-4.6	0.7	
	1	-	10.19	B3LYP/6-311G(d,p)	-103.5	-4.5	-2.2	0.2	
	1	-	5.03	B3LYP/6-311G(d,p)	9.4	-3.3	-3.3	1.3	
	1	-	4.73	B3LYP/6-311G(d,p)	-3.2	-2.7	-7.7	24.5	
	1	-	5.84	B3LYP/6-311G(d,p)	-3.5	-5.7	-4.3	9.8	
	1	-	6.43	B3LYP/6-311G(d,p)	12.3	-3.8	-2.1	0.5	
	1	-	6.31	B3LYP/6-311G(d,p)	9.9	-3.0	-1.5	0.2	
	1	-	5.66	B3LYP/6-311G(d,p)	11.6	-1.4	-1.3	0.1	

	1	-	6.71	B3LYP/6-311G(d,p)	-209.9	-18.7	-10.9	11.3	
	1	-	3.51	B3LYP/6-311G(d,p)	-266.3	-39.9	-45.7	35.9	
	1	-	7.27	B3LYP/6-311G(d,p)	-479.2	-102.9	-14.1	138.4	
	1	-	8.92	B3LYP/6-311G(d,p)	-184.8	-8.9	-1.2	0.0	

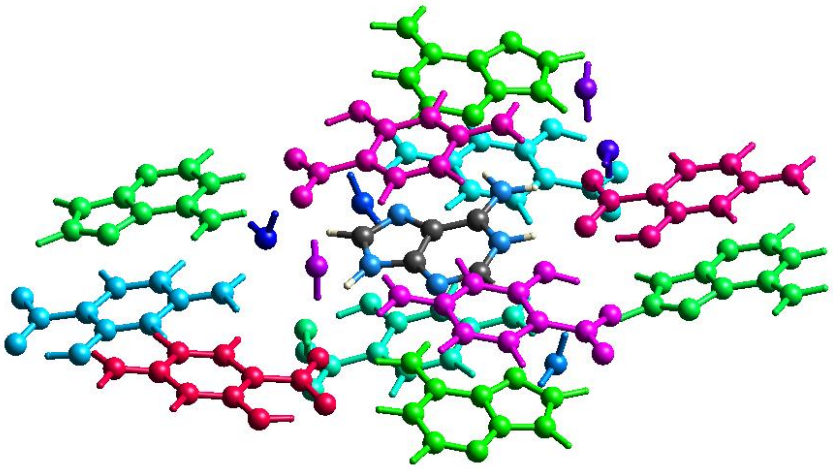

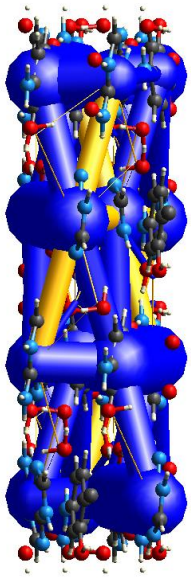

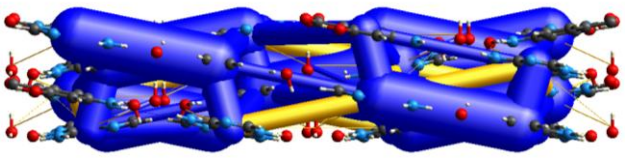

a) b)

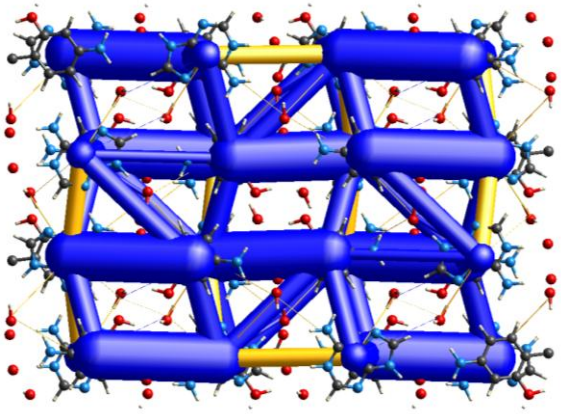

c)

Figure S9 - Total Energy component of Energy Framework of Form C along [100] (a), [010] (b) and [001] (c) (Color code: blue, attractive; yellow, repulsive).

a)

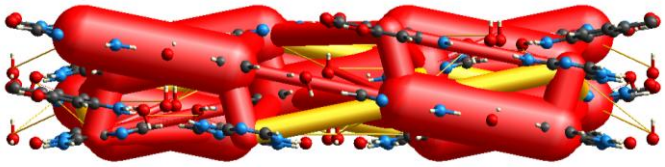

b)

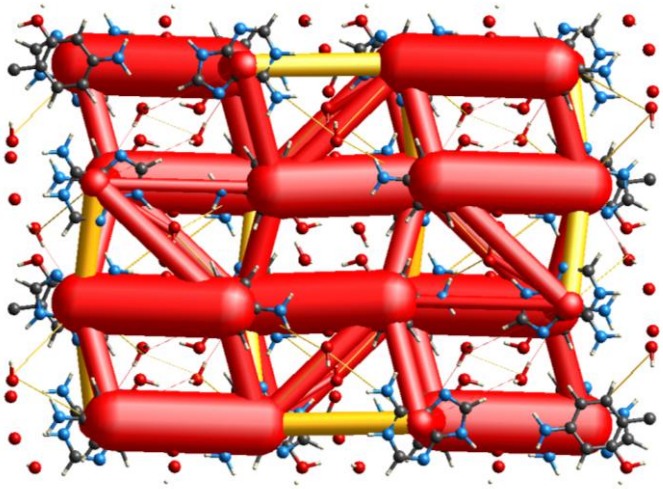

c)

Figure S10 - Coulombic component of Energy Framework of Form C along [100] (a), [010] (b) and [001] (c) (Color code: red, attractive; yellow, repulsive).

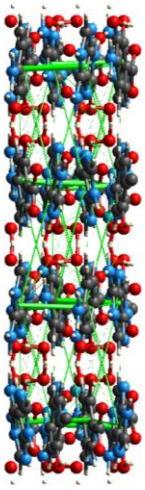

a)

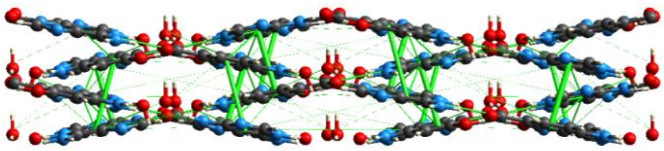

b)

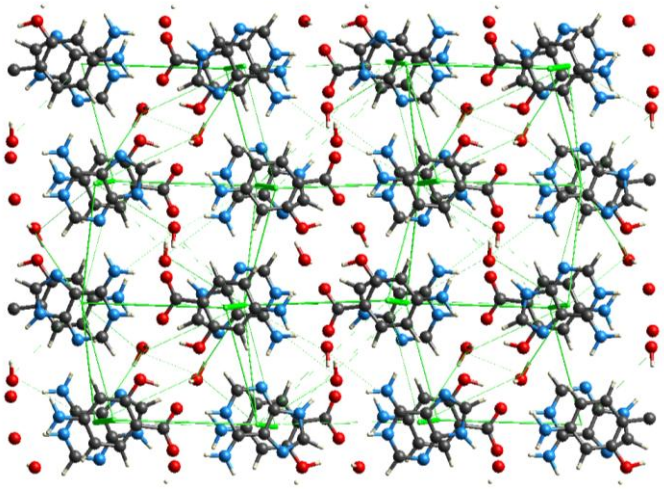

c)

Figure S11 - Dispersion component of Energy Framework of Form C along [100] (a), [010] (b) and [001] (c).

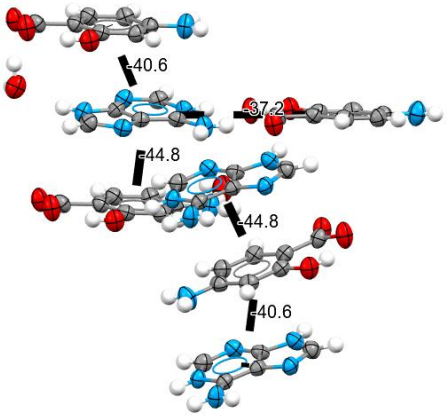

a)

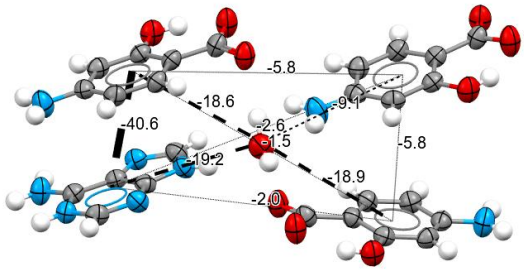

O5

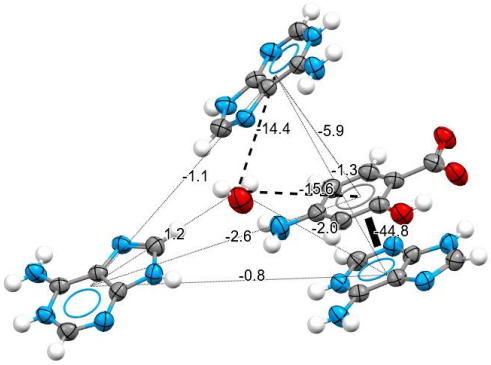

O4

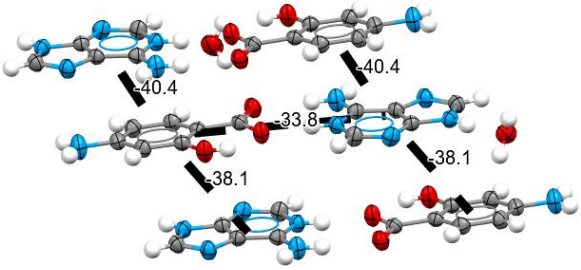

b)

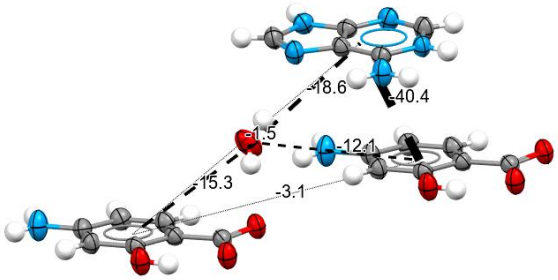

O4

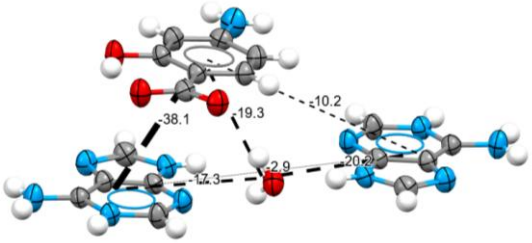

O5

Figure S12 - Fragments of the crystal packing with the interaction energetic components in KJ/mol calculated with the Mercury feature for Form B (a) and Form C (b) (Ellipsoid probability: 70%). Color code: grey, carbon; blue, nitrogen; red, oxygen; white, hydrogen.

Table S8 - ^{13}C and ^{15}N chemical shift assignments for a) starting materials and b) the three polymorphs: Form A, B and C.

a)

PAS			ADE		
atom	group	ppm	atom	group	ppm
^{13}**C**			^{13}**C**		
7	**C**OOH	176.3	6’	**C**OOH	156.1
2	**C**(Ar)-OH	163.1	2’	**C**(Ar)-OH	149.5
4	**C**(Ar)-NH_2	155.7	4’	**C**(Ar)-NH_2	149.5
6	**C**(Ar)-H	135.9	8’	**C**(Ar)-H	137.3
1	**C**(Ar)-COOH	108.2	5’	**C**(Ar)-COOH	117.4
3	**C**(Ar)-H	99			
5	**C**(Ar)-H	99			
^{15}**N**			^{15}**N**		
11	**N**H_2	62	7’	**N**(Ar)	233.9
			1’	**N**(Ar)	225.4
			3’	**N**(Ar)	214.7
			9’	**N**(Ar)-H	159.4
			10’	**N**H_2	90.3

b)

Form A			Form B			Form C		
atom	group	ppm	atom	group	ppm	atom	group	ppm
^{13}C			^{13}C			^{13}C		
7	**C**OOH	175.2-174.3-173.3	7	**C**OOH	177.3	7	**C**OOH	177.7
2	**C**(Ar)-OH	163.4-162.1	2	**C**(Ar)-OH	161.8	2	**C**(Ar)-OH	162.4
4/4'/6'	**C**(Ar)-NH_2/ **C**(Ar)/ **C**(Ar)-NH_2	155.4-149.9-148.6	4/2'/4'/6'/8'	**C**(Ar)-NH_2/ **C**(Ar)-H/ **C**(Ar)/ **C**(Ar)-NH_2/ **C**(Ar)-H	153.2-151.4-149.6-148.1-145.1-142.8	4/2'/4'/6/8'	**C**(Ar)-NH_2/ **C**(Ar)-H/ **C**(Ar)/ **C**(Ar)-NH_2/ **C**(Ar)-H	152-151.5-149.1-144.7
2'	**C**(Ar)-H	152.9-151	6	**C**(Ar)-H	130.2	6	**C**(Ar)-H	132.5
8'	**C**(Ar)-H	143.7-138.6	5'	**C**(Ar)	118.1	5'	**C**(Ar)	118.4
6	**C**(Ar)-H	132.9	1/3/5	**C**(Ar)-COOH/ **C**(Ar)-H/ **C**(Ar)-H	104.5-98.7	1/3/5	**C**(Ar)-COOH/ **C**(Ar)-H/ **C**(Ar)-H	107.3-106-98.3
5'	**C**(Ar)	119.2-117.3						
3/5	**C**(Ar)-H/ **C**(Ar)-H	108.4-101.2-99.5-98.2						
1	**C**(Ar)-COOH	107.4-103.7-102.3						
^{15}N			^{15}N			^{15}N		
7'/1'/3'	**N**(Ar)	237.9-223.2-216.8-215.5-207.4	7'/3'	**N**(Ar)	234.2-216.8	7'/3'	**N**(Ar)	233.6-218.4
9'	**N**(Ar)-H	163.3-155.6	1'/9'	**N**(Ar)/ **N**(Ar)-H	157.8-156	1'/9'	**N**(Ar)/ **N**(Ar)-H	160.5-154.3
10'	$\mathbf{NH_2}$	82.8-77.5	10'/11	$\mathbf{NH_2}$/$\mathbf{NH_2}$	84.9-61.5	10'/11	$\mathbf{NH_2}$	83.7-47.4
11	$\mathbf{NH_2}$	68.1-67-65.5						

Section S1 – Signal assignments of ^{15}N CPMAS SSNMR:

For each Form the signals in ^{15}N spectra are consistent with the stoichiometry of the polymorphs: 3:2 PAS:ADE for Form A, and 1:1:2 PAS:ADE:H_2O for Forms B and C. Form A shows two distinct peaks for both N10' and N9' compared to pure ADE, confirming the presence of two ADE molecules in the unit cell of the adduct. The aliphatic region further exhibits the contribution of N10 of PAS with three partially overlapping signals. Five signals (one with double integral value) corresponding to N7', N1', and N3' appear between 240-202 ppm in agreement with the presence of three independent molecules of ADE. By contrast, Forms B and C display only two signals in the 234-219 ppm region. This evidence confirms that N1' (as established by SCXRD) participates in a charge-transfer hydrogen bond, resulting in its signal shifting toward lower frequencies near the N9' signal (157.8-156 ppm for Form B and 160.5-154.3 ppm for Form C). The aliphatic region (100-50 ppm) shows two signals, attributed to N10' and N11.

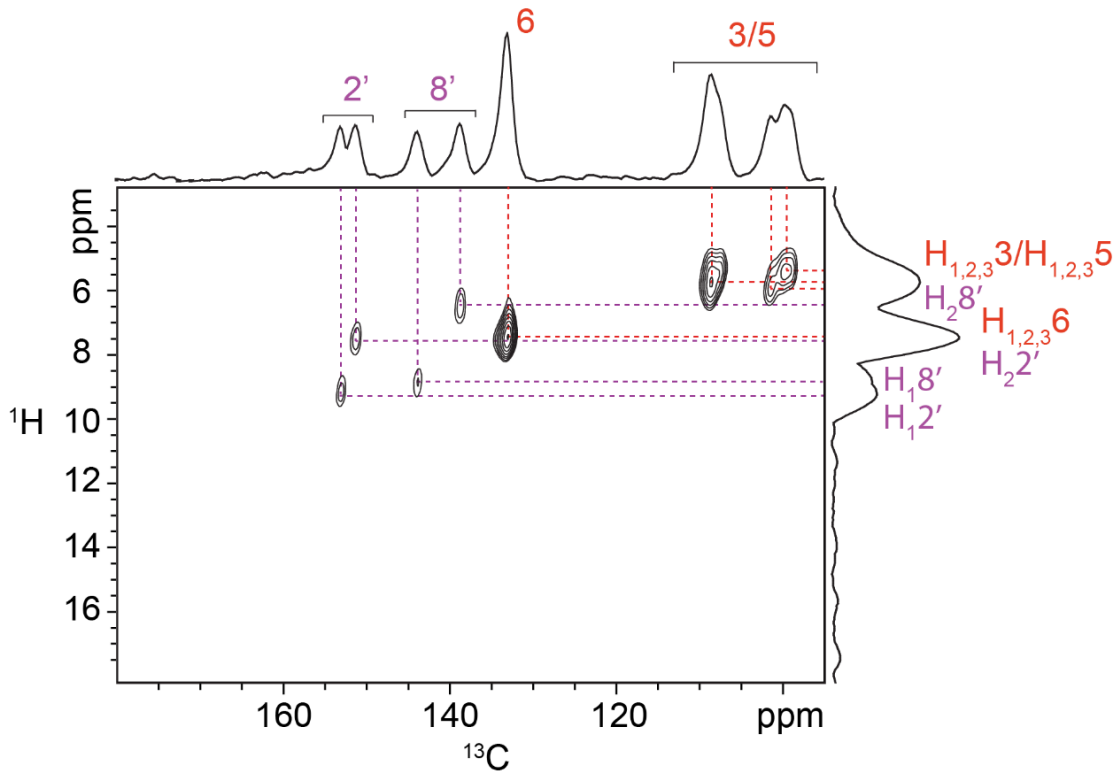

Figure S13 – ^1H–^{13}C 2D CP FSLG HETCOR "short range" (contact time = 0.1 ms) spectrum of Form A recorded at room temperature at 12 kHz. Purple signals and dashed lines highlight carbon atoms covalently bonded to hydrogen atoms of the two molecules of ADE, whereas red signals and dashed lines highlight those of the three molecules of PAS.

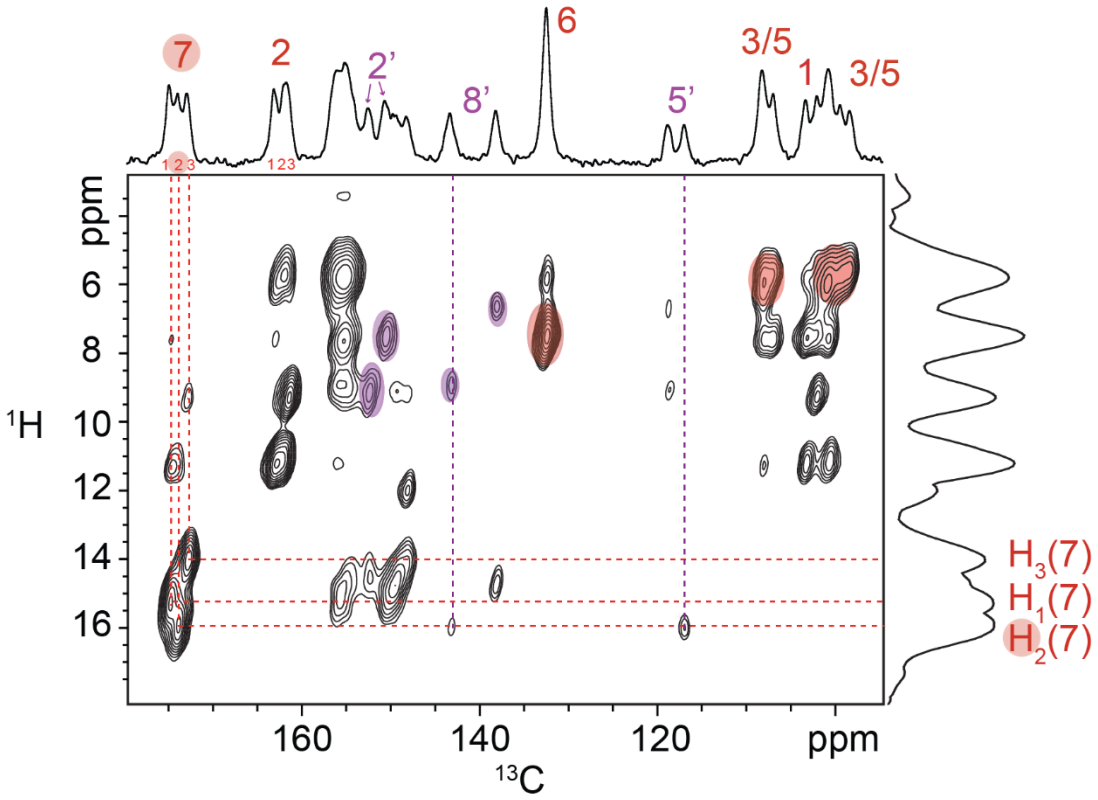

Figure S14 - $^{1}H–^{13}C$ 2D CP FSLG HETCOR "long range" (contact time = 2.5 ms) spectrum of Form A recorded at room temperature at 12 kHz. Colored correlations refer to short range proximities, i.e. directly bonded C-H pairs, as observed in the $^{1}H–^{13}C$ 2D CP FSLG HETCOR "short range" spectrum. Red dashed lines highlight correlations involving the carboxylic carbon of PAS, while purple dashed lines underline the correlations of the carboxylic proton of $C7_2$ (PAS) to the C8' and C5' carbons of ADE.

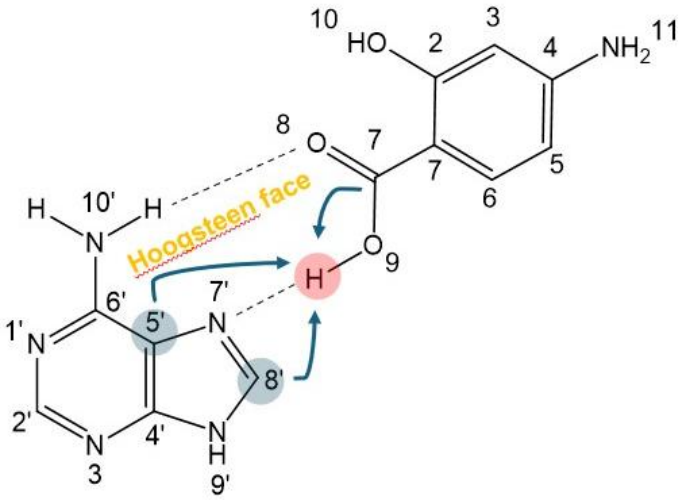

Figure S15 – Representation of one the possible synthons between the PAS carboxyl group and the Hoogsteen face of ADE in Form A as deducted from the $^{1}H–^{13}C$ 2D CP FSLG HETCOR "long range" spectrum. The blue arrows indicate carbon-hydrogen proximities observed in the $^{1}H–^{13}C$ 2D CP FSLG HETCOR "long range" spectrum.

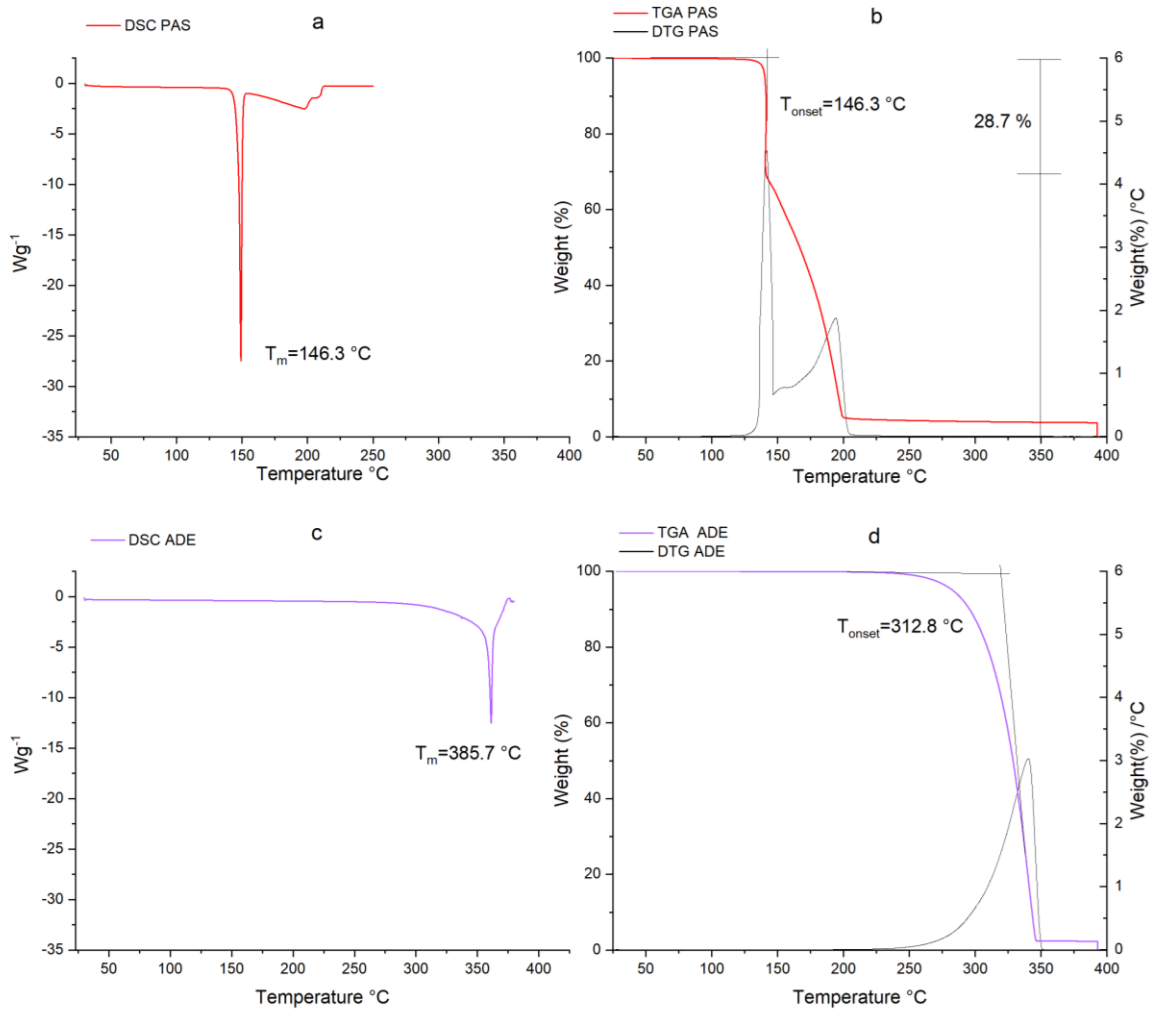

Figure S16 – DSC and TGA profiles of starting materials: PAS (a,b) and ADE (c,d). DSC thermograms show melting temperatures (T_m), while TGA traces include onset temperatures (T_{onset}).

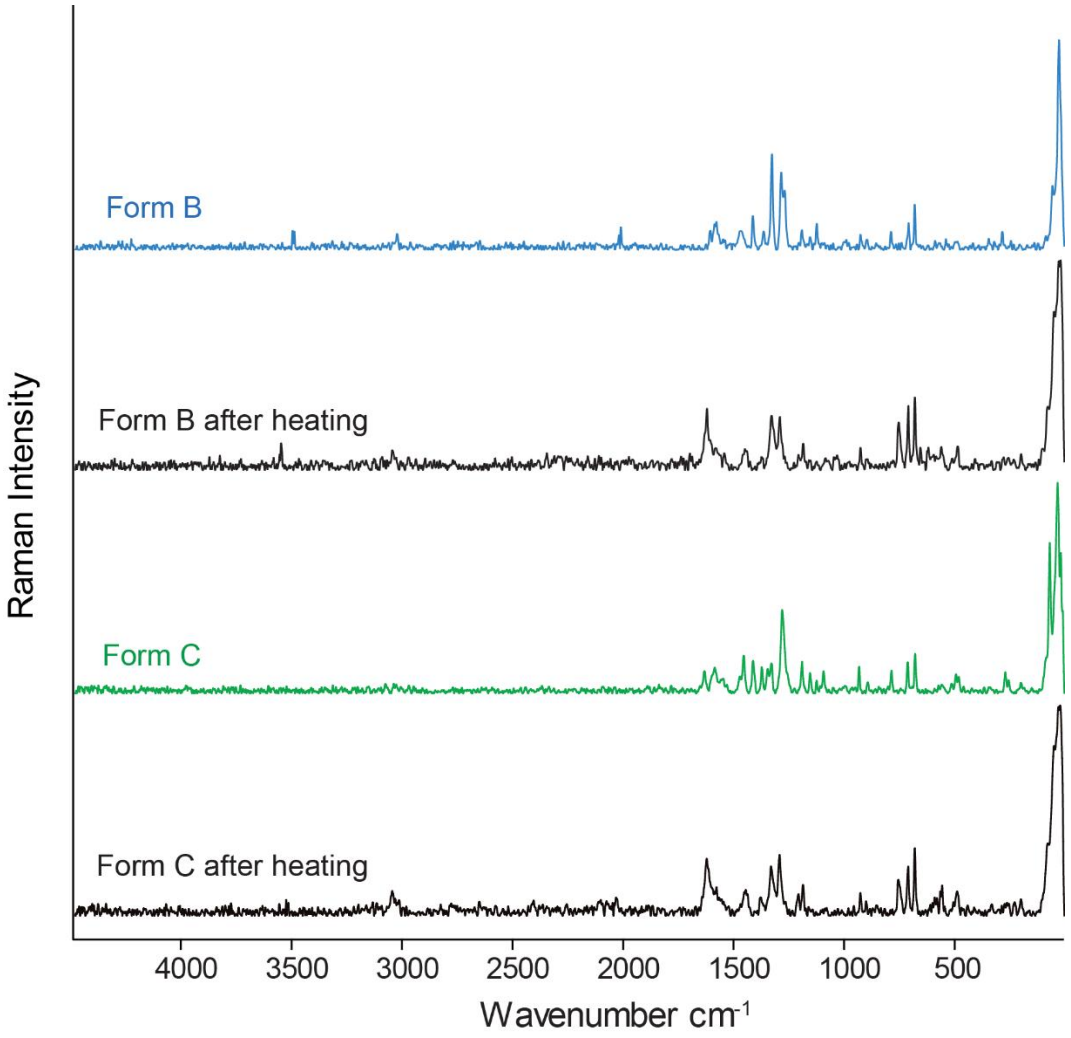

Figure S17 - Raman spectra of Form A, Form B, and Form B and Form C after heating (30 min at 100°C).

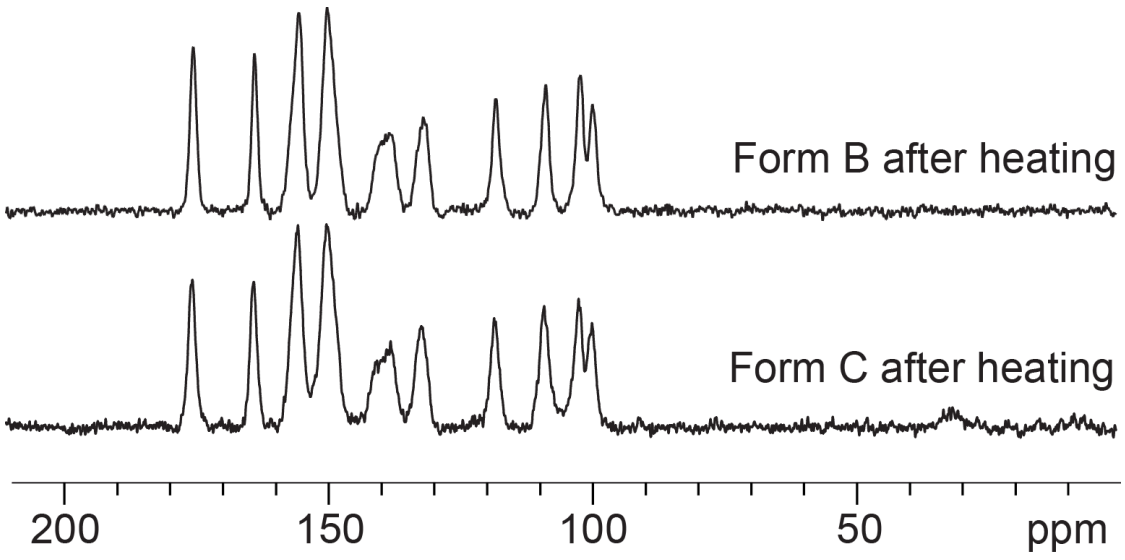

Figure S18 – Comparison of the ^{13}C (100.91 MHz) CPMAS SSNMR spectra of Forms B and C after heating. Spectra were recorded at 12 kHz MAS and room temperature.

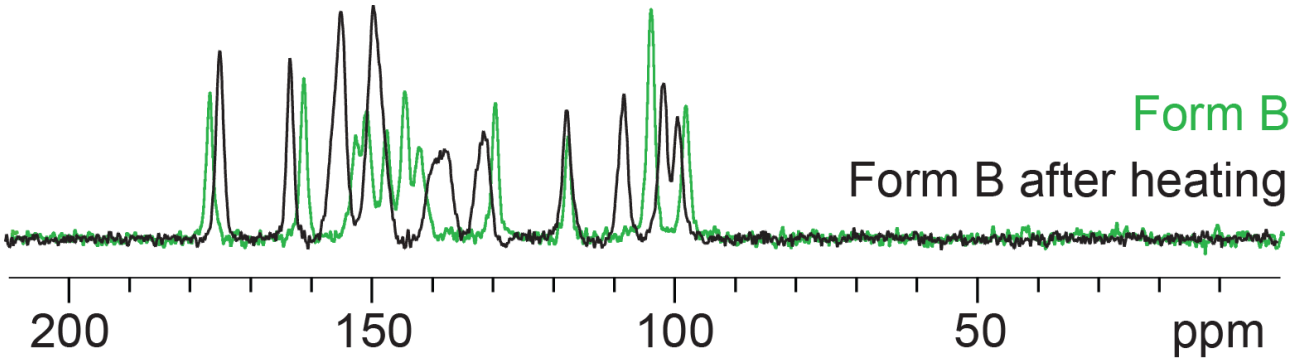

Figure S19 - Comparison of the ^{13}C (100.63 MHz) CPMAS SSNMR spectra of Form B and ^{13}C (100.91 MHz) CPMAS SSNMR Form B after heating. Spectra were recorded at 12 kHz MAS and room temperature.

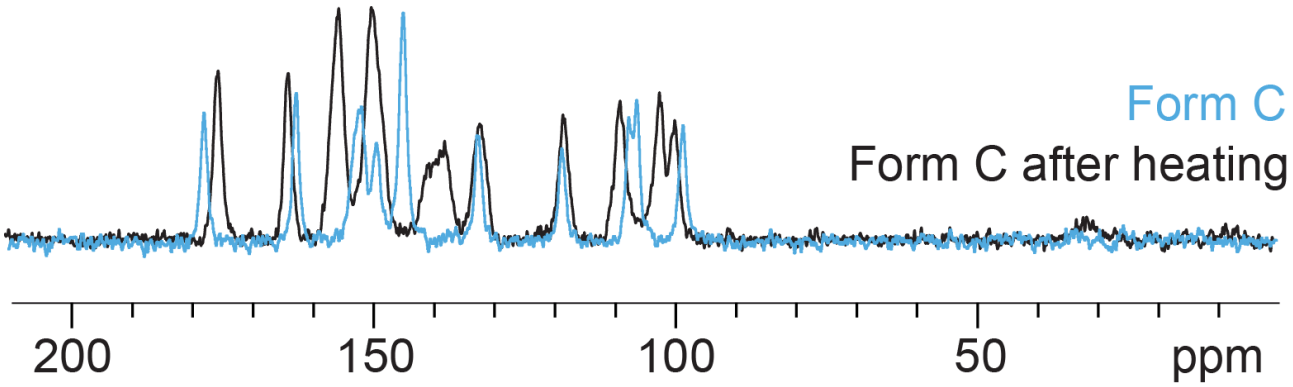

Figure S20 - Comparison of the ^{13}C (100.63 MHz) CPMAS SSNMR spectra of Form C and ^{13}C (100.91 MHz) CPMAS SSNMR Form C after heating. Spectra were recorded at 12 kHz MAS and room temperature.

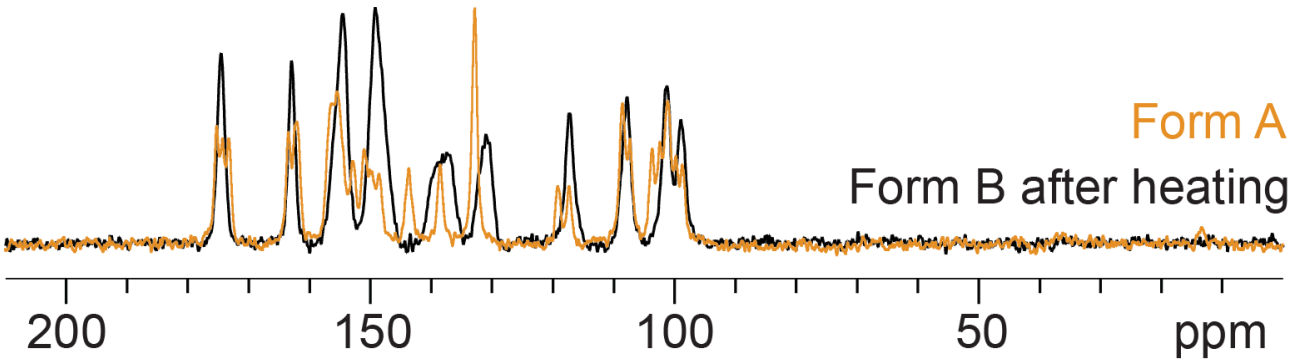

Figure S21 - Comparison of the ^{13}C (100.63 MHz) CPMAS SSNMR spectra of Form A and ^{13}C (100.91 MHz) CPMAS SSNMR Form B after heating. Spectra were recorded at 12 kHz MAS and room temperature.

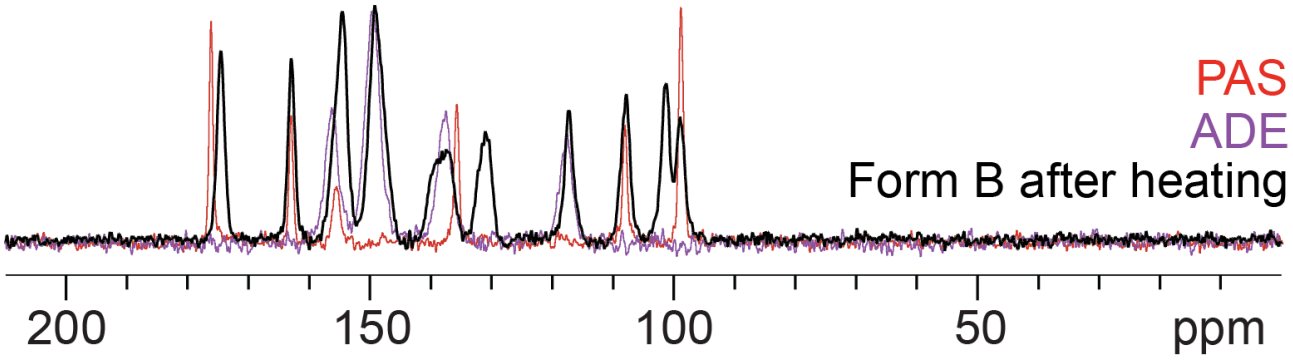

Figure S22 - Comparison of the ^{13}C (100.63 MHz) CPMAS SSNMR spectra of starting materials and ^{13}C (100.91 MHz) CPMAS SSNMR Form B after heating. Spectra were recorded at 12 kHz MAS and room temperature.

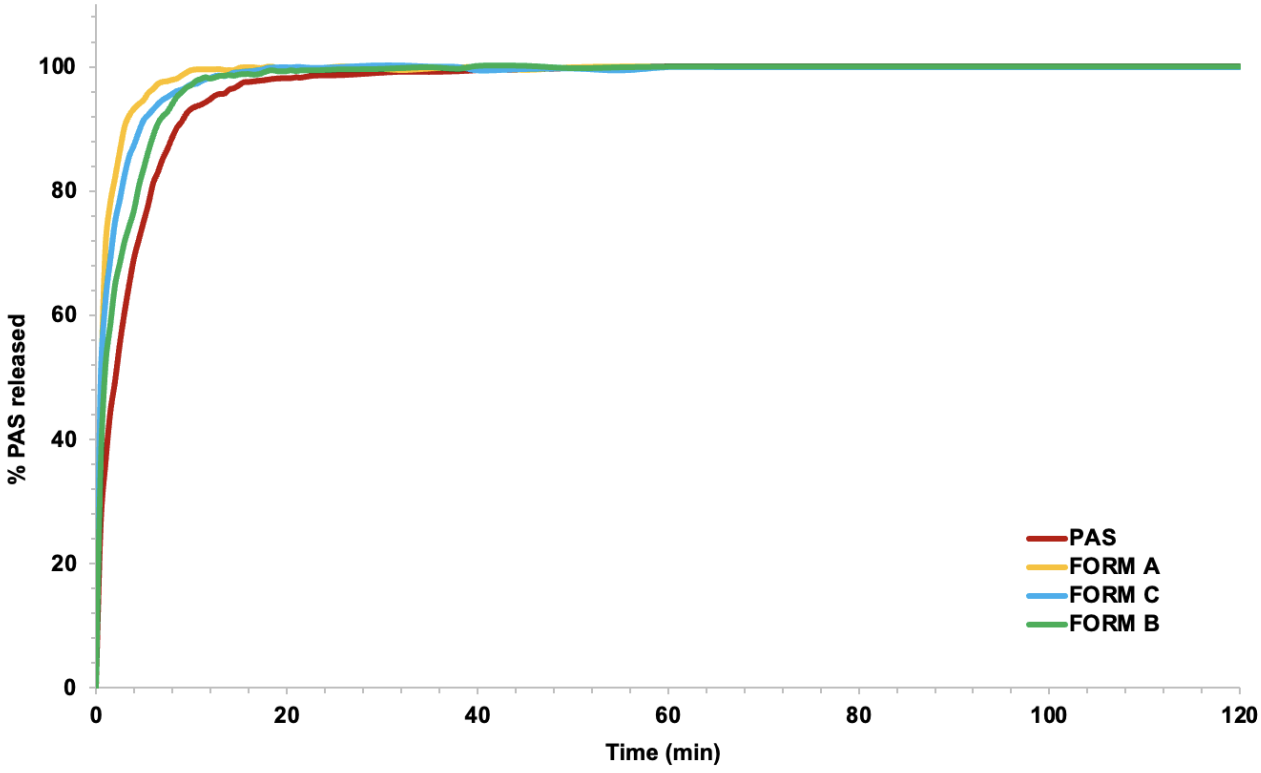

Figure S23 – Complete 2-hour dissolution profiles of pure PAS (red) and the three adducts: Form A (yellow), Form B (green) and Form C (light blue), expressed as % of PAS released. Profiles represent the average of three replicates, with standard deviations not exceeding 5% of the mean value.